EINDHOVEN UNIVERSITY OF TECHNOLOGY

B-spline parametrization of the dielectric function applied to spectroscopic ellipsometry on amorphous carbon

Citation for published version (APA):
Weber, J. W., Hansen, T. A. R., Sanden, van de, M. C. M., & Engeln, R. A. H. (2009). B-spline parametrization of the dielectric function applied to spectroscopic ellipsometry on amorphous carbon. *Journal of Applied Physics*, *106*(12), 123503-1/9. Article 123503. https://doi.org/10.1063/1.3257237

DOI:
10.1063/1.3257237

Document status and date:
Published: 01/01/2009

Document Version:
Publisher's PDF, also known as Version of Record (includes final page, issue and volume numbers)

Please check the document version of this publication:

• A submitted manuscript is the version of the article upon submission and before peer-review. There can be important differences between the submitted version and the official published version of record. People interested in the research are advised to contact the author for the final version of the publication, or visit the DOI to the publisher's website.
• The final author version and the galley proof are versions of the publication after peer review.
• The final published version features the final layout of the paper including the volume, issue and page numbers.

Link to publication

General rights
Copyright and moral rights for the publications made accessible in the public portal are retained by the authors and/or other copyright owners and it is a condition of accessing publications that users recognise and abide by the legal requirements associated with these rights.

• Users may download and print one copy of any publication from the public portal for the purpose of private study or research.
• You may not further distribute the material or use it for any profit-making activity or commercial gain
• You may freely distribute the URL identifying the publication in the public portal.

If the publication is distributed under the terms of Article 25fa of the Dutch Copyright Act, indicated by the "Taverne" license above, please follow below link for the End User Agreement:

www.tue.nl/taverne

Take down policy
If you believe that this document breaches copyright please contact us at:

openaccess@tue.nl

providing details and we will investigate your claim.

Download date: 04. Oct. 2023

B-spline parametrization of the dielectric function applied to spectroscopic ellipsometry on amorphous carbon

J. W. Weber, T. A. R. Hansen,[a] M. C. M. van de Sanden, and R. Engeln[b]
Department of Applied Physics, Eindhoven University of Technology, P.O. Box 513, 5600 MB Eindhoven, The Netherlands

(Received 14 July 2009; accepted 27 September 2009; published online 16 December 2009)

The remote plasma deposition of hydrogenated amorphous carbon (a-C:H) thin films is investigated by *in situ* spectroscopic ellipsometry (SE). The dielectric function of the a-C:H film is in this paper parametrized by means of B-splines. In contrast with the commonly used Tauc–Lorentz oscillator, B-splines are a purely mathematical description of the dielectric function. We will show that the B-spline parametrization, which requires no prior knowledge about the film or its interaction with light, is a fast and simple-to-apply method that accurately determines thickness, surface roughness, and the dielectric constants of hydrogenated amorphous carbon thin films. Analysis of the deposition process provides us with information about the high deposition rate, the nucleation stage, and the homogeneity in depth of the deposited film. Finally, we show that the B-spline parametrization can serve as a stepping stone to physics-based models, such as the Tauc–Lorentz oscillator. © *2009 American Institute of Physics*. [doi:10.1063/1.3257237]

I. INTRODUCTION

The chemical inertness, low to high nanohardness, and thermal and conductive properties of hydrogenated amorphous carbon (a-C:H) thin films allow them to be used in a wide variety of applications, ranging from the microchip industry to protective (e.g., optical windows and magnetic storage disks) and biomedical coatings.[1,2] Remote plasma deposition is used to deposit, among others, diamondlike carbon films with a nanohardness in excess of 13 GPa at high deposition rates (>10 nm/s), while maintaining good adhesion and chemical stability (see, e.g., Refs. 1, 3, and 4, and references therein).

In this paper, remote plasma deposition of hydrogenated amorphous carbon (a-C:H) thin films is investigated by *in situ* spectroscopic ellipsometry (SE). SE is a noninvasive optical diagnostic that can measure the change in polarization of light reflected on a thin film.[5–7] This change in polarization is determined by the ratio of the Fresnel reflection coefficients for both p- and s-polarized light, commonly expressed as $\rho = r_p / r_s = \tan \Psi e^{i\Delta}$. Determining the dielectric function ($\varepsilon = \varepsilon_1 + i\varepsilon_2$) from the measured SE data requires a (multilayered) model that describes the interaction of the incident light with the film. The dielectric spectrum of an a-C:H film (see Fig. 1) is characterized by the π-π^* electronic transition around 4 eV and the σ-σ^* electronic transition around 13 eV.[8–10] In SE studies of these films, each transition is commonly modeled by a Tauc–Lorentz (TL) oscillator.[8,9,11] However, the majority of standard spectroscopic ellipsometers are not capable of reaching 13 eV or above, necessitating the use of complementary diagnostics, e.g., electron energy loss spectroscopy.[12,13] *In situ* measurements with such complementary diagnostics during film growth are in most cases, such as ours, practically not feasible. Also the (in)homogeneity in depth of the carbon film, which is not always known, needs to be taken into account in the optical model. For all these reasons, it is therefore not always possible to apply a model based on two TL oscillators to the measured SE data.

Even when two TL oscillators could be used, it is not necessary to apply such a physics-based model if only the — evolution in — thickness and roughness (i.e., growth rate and nucleation) and an accurate parametrization of the dielectric function of the thin film are of interest to the experimentalist. The approach in this paper, therefore, is to obtain a purely mathematical and Kramers–Kronig consistent parametrization of the dielectric function by means of B-splines.[14] Such a parametrization of the deposited carbon layer requires no prior knowledge about the film properties or assumptions about the interaction of light with the film. The optical model for our films consists of a substrate, the

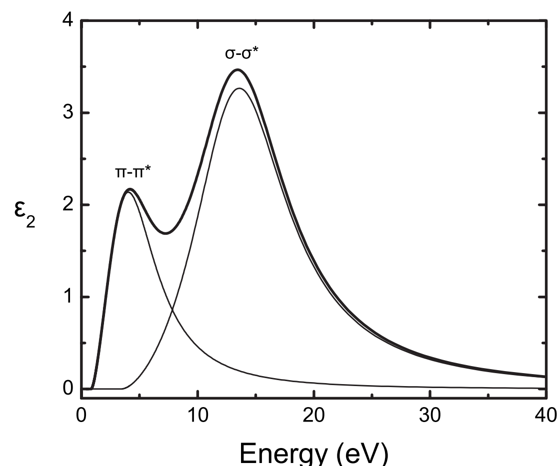

FIG. 1. Wide range ε_2 spectrum for a-C:H, as simulated by two TL oscillators. The parameters for the π-π^* transition are $A_\pi = 19.5$ eV, $\Gamma_\pi = 6.35$ eV, $E_{0,\pi} = 4.55$ eV, and $E_{g,\pi} = 0.82$ eV; and for the σ-σ^* transition $A_\sigma = 57.2$ eV, $\Gamma_\sigma = 10.1$ eV, $E_{0,\sigma} = 13.9$ eV, and $E_{g,\sigma} = 3.37$ eV.

[a]Electronic mail: t.a.r.hansen@tue.nl.
[b]Electronic mail: r.engeln@tue.nl.

 © 2009 American Institute of Physics

Downloaded 25 Mar 2010 to 131.155.110.244. Redistribution subject to AIP license or copyright; see http://jap.aip.org/jap/copyright.jsp

bulk of the film itself, and a roughness layer, whereby each layer is defined by its own thickness and dielectric constants. While the dielectric function of the bulk layer is represented by B-splines, the roughness is modeled by Bruggeman's effective medium approximation (EMA) of 50% bulk material and 50% voids.[15] This layer structure, whereby the bulk carbon material is parametrized by means of B-splines, is hereafter referred to as the B-spline model. An ideal fit between model and data would give a value close to 1 for the unbiased maximum likelihood estimator χ^2. Large deviations from 1 could indicate an incorrect or incomplete model. However, it can also point to the accumulation of very small experimental errors in the obtained data.[7] A model can quickly grow in complexity, while still reducing the overall χ^2 due to an increase in the number of fitting parameters. Therefore, we verify the validity of the layer structure of the B-spline model for our carbon films by complementary experimental techniques, i.e., atomic force microscopy (AFM) and cross-sectional scanning electron microscopy (SEM) measurements. In addition to verifying the layer structure, we will also compare the B-spline parametrization — of an *ex situ* measurement — with a wavelength-by-wavelength fit.

In situ measurements, also analyzed by the B-spline model, are used to calculate the deposition rate and to investigate the nucleation of the film. Although other methods — e.g., single wavelength ellipsometry[16] — are available to determine the film thickness during deposition, *in situ* SE and, in particular, the B-spline model have the advantage that the dielectric function can be accurately determined without the need for any assumptions about the film's interaction with light. This will allow us to establish the (in)homogeneity in depth of the deposited layer. We will also show that the B-spline parametrization of the dielectric function can also serve as a stepping stone to a parametrization with a TL oscillator. Finally, the dielectric spectra of the *a*-C:H film in both vacuum and ambient air are tabulated in this paper by means of B-splines.

II. EXPERIMENTAL SETUP

A. Reactor

Hydrogenated amorphous carbon thin films are deposited on a 1 mm thick silicon wafer with a 1.6 nm native oxide layer. The plasma source (see Fig. 2) used for deposition is a cascaded arc consisting of a stack of four water cooled copper plates with a 4 mm central arc channel.[17,18] A dc of 75 A runs from three tungsten cathodes, through the arc channel, to the anode plate at the end. This current creates an Ar plasma (100 sccs) under high pressure (540 mbars) that expands supersonically into a low pressure reactor (30 Pa). After formation of a shock zone, the plasma continues subsonically toward the substrate holder, located at around 55 cm from the exit of the arc. The substrate temperature is kept at a constant 250 °C throughout the 25–40 s deposition time, which is controlled by the opening and (automatic) closing of the shutter. A He backflow of 1 sccs is used for improved thermal contact between the substrate holder and the sample.[19]

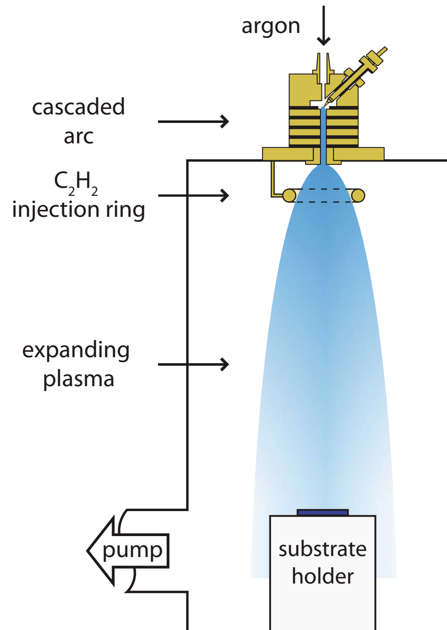

FIG. 2. (Color online) A schematic cross section of the deposition setup.

The reactor is equipped with a load lock, a shutter to avoid direct exposure of the sample to the plasma jet, and access ports for SE with a fixed angle of incidence of 68°. During *ex situ* SE measurements the angle of incidence is 70°. The precursor, 15 sccs of acetylene (C_2H_2), is injected through a ring, which is located 5 cm from the exit of the plasma source. The dissociation of the precursor occurs in the expanding plasma jet through charge transfer and dissociative recombination with the Ar ions and electrons, respectively. This ion chemistry results in a high radical flux toward the surface, which causes a high deposition rate.[3]

B. Spectroscopic Ellipsometry

The *in situ* experiments are performed with a spectroscopic ellipsometer measuring in the visible and near infrared wavelength ranges (0.75–5.0 eV, J. A. Woollam Co., Inc. M2000U), whereas the deposited samples are characterized *ex situ* for the visible and ultraviolet wavelength ranges (1.2–6.5 eV, J. A. Woollam Co., Inc. M2000D). Both ellipsometers are rotating compensator ellipsometers. The data acquisition rate of the ellipsometer is set to 200 rev/measurement for the *ex situ* measurement, with the high accuracy mode enabled. This indicates that each measurement is the average of 200 revolutions of the compensator. To obtain the highest acquisition rate for the *in situ* measurements, 1 rev/measurement without the high accuracy mode is used. The actual number of rev/measurement, over which is averaged, depends on the processing power of the computer. Although this number is not included in the data file, it can be determined from the acquisition time between two datapoints.[20] The analysis software is WVASE32 3.668 and CompleteEASE 3.55 and 4.06, from J. A. Woollam Co., Inc.

Downloaded 25 Mar 2010 to 131.155.110.244. Redistribution subject to AIP license or copyright; see http://jap.aip.org/jap/copyright.jsp

1. Layer structure

Each optical model, used for the analysis of SE data, has a layer structure whereby each layer is defined by its own thickness and dielectric constants. A three-tiered layer structure is used for the *a*-C:H thin films investigated in this paper. The first layer is a 1 mm thick silicon wafer with a 1.6 nm native oxide layer. The native oxide layer was measured prior to deposition, and both thicknesses are fixed in the layer model. This is the substrate on which amorphous carbon, i.e., the second layer, is deposited. The third and last layer is the roughness, which is modeled by Bruggeman's EMA of 50% bulk material and 50% voids.[15] The (in)homogeneity in depth of the carbon layer is discussed in Sec. III C. This fairly simple and straightforward layer structure is used for the B-spline model, in which the dielectric function of the carbon layer is parametrized by means of B-splines.

2. B-splines

Basis-splines, commonly abbreviated to B-splines, are a recursive set of polynomial splines

$$B_i^0(x) = \begin{cases} 1, & t_i \leq x \leq t_{i+1} \\ 0 & \text{otherwise}, \end{cases} \tag{1a}$$

$$B_i^k(x) = \left(\frac{x - t_i}{t_{i+k} - t_i}\right) B_i^{k-1}(x) + \left(\frac{t_{i+k+1} - x}{t_{i+k+1} - t_{i+1}}\right) B_{i+1}^{k-1}(x), \tag{1b}$$

where k is the degree of the B-spline and i is the index for the knots t_i that denote the position, on the x-axis, where the polynomial segments connect.[14] The total spline curve $S(x)$, representing the dielectric function of the film layer, is then given by

$$S(x) = \sum_{i=1}^{n} c_i B_i^k(x), \tag{2}$$

with c_i the B-spline coefficients. $(t_{i+2},\ c_i)$ denote the locations of the control points of the B-spline curve. If there are n knots then there are $n-k-1$ control points, i.e., the last control point is located at $(t_{n-k+1},\ c_{n-k-1})$. CompleteEASE uses cubic B-splines $(k=3)$. With $k=3$, each control point influences only the two previous and the following two polynomial segments.[21] This is known as local support.[14]

The number of coefficients used to accurately describe the dielectric function should be kept as low as possible, while still adhering to the shape of the function. Although additional coefficients can provide a better description, too large a number leads to an unrealistic result in which only the noise is better described. It also increases the possibility of correlation between the coefficients.

B-splines can be ensured to have a physical meaning because of the following two properties. First, a Kramers–Kronig transform exists of a B-spline curve, i.e., ε_1 can be found from a Kramers–Kronig transformation of ε_2. This reduces the number of fitting parameters by two and therefore also reduces the probability of correlation between them. Kramers–Kronig consistency requires that ε_2 goes smoothly to zero. This is ensured by choosing knots at appropriate locations outside the measured range. These outer knots should, therefore, also be communicated. Second, B-splines have a property known as *convex hull*[14]: if all coefficients c_i are positive then the total curve is also positive. Since ε_2 can never be negative, all c_i's should be positive. By enforcing that the B-spline curve is Kramers–Kronig consistent and that all c_i's are positive, a physical result for the parametrized dielectric function is ensured. Both conditions are enforced for all the B-spline parametrizations in this work.

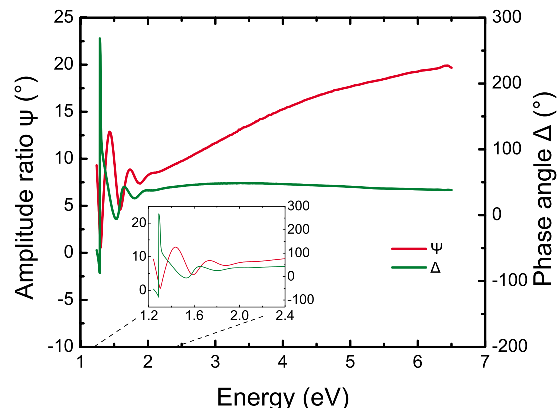

FIG. 3. (Color online) *Ex situ* measurement of Ψ and Δ as a function of energy, which is a common representation of SE data. A film thickness and surface roughness of, respectively, 940 and 6 nm are derived for this *a*-C:H film by means of a Cauchy model.

3. The Cauchy model

Hydrogenated amorphous carbon thin films are semitransparent, as is evident from the interference fringes in the long wavelength region in Fig. 3. The transparent part can be fitted by empirical Cauchy dispersion relation (3a) for the refractive index.[5,22] The Cauchy dispersion relation by itself is not Kramers–Kronig consistent, since ε_2 is assumed to be zero. However, absorptions can be accounted for by adding relation (3b) to the dispersion relation

$$n(E) = A + BE^2 + CE^4, \tag{3a}$$

$$k(E) = De^{F(E-E_{\text{edge}})}, \tag{3b}$$

with A, B, C, D, and F the fitting parameters and E_{edge} the band edge.[5,22] Both relations together are hereafter referred to as the Cauchy model. Good estimates for thickness and roughness are found from this model. After determining the thickness and roughness from the transparent part of the data, the optical constants for the entire spectrum, including the absorbing part, can be found by an exact direct numerical inversion. This inversion is carried out wavelength by wavelength. Due to noise in the experimental data, it is not guaranteed that the dielectric function, resulting from the numerical inversion, is indeed Kramers–Kronig consistent.

4. Tauc-Lorentz oscillator

A Kramers–Kronig consistent parametrization of ε_2 by the TL oscillator is given by

Downloaded 25 Mar 2010 to 131.155.110.244. Redistribution subject to AIP license or copyright; see http://jap.aip.org/jap/copyright.jsp

TABLE I. Sample list.

Section	Sample
III A: Cauchy model	A
III B: The dielectric function in ambient air	A
III C: Growth rate and homogeneity	B
III D: TL oscillator	A

$$\varepsilon_2 = \begin{cases} \dfrac{AE_0\Gamma(E-E_g)^2}{E[(E^2-E_0^2)^2+\Gamma^2E^2]}, & E \geq E_g \\ 0, & E < E_g, \end{cases} \quad (4)$$

where E_g is the Tauc gap for amorphous materials and $A = e^2N_e/\varepsilon_0 m_e$ is for the total number of electrons N_e with mass m_e, ε_0 the dielectric constant in vacuum, and elementary charge e.[5,11] The amplitude of the oscillator is $A/\Gamma E_0$, which has its maximum at E_0, and Γ represents the full width, half maximum.

5. Pole

In the last part of the experimental results, *ex situ* data will be analyzed by a TL oscillator in combination with a pole. This is a Lorentz oscillator without broadening

$$\varepsilon_{\text{pole}} = \frac{A}{E_{\text{pole}}^2 - E^2}, \quad (5)$$

with amplitude A at an energy position E_{pole}. The pole, which affects only ε_1 of the dielectric function, takes absorptions outside the measured range (see Sec. III D) into account.[22] Because A and E_{pole} are susceptible to correlation, the *global fit* option of CompleteEASE is used. A global fit divides the parameter space into a grid of starting values for the fitting procedure. The parameters we used for the global fit itself are 20 iterations for each set of starting values and a limitation of the measured data to 100 datapoints. The set of starting values with the lowest χ^2 is subsequently used for an extensive fit. Compared to the B-spline method, a global fit of a pole is computationally much more demanding and thus takes a longer time to complete. Despite the higher computational requirements of a pole, it does give a physical representation of absorptions outside the measured range.

III. EXPERIMENTAL RESULTS

The experimental results are elucidated by means of two samples (see Table I). Sample A is used for the *ex situ* results in Secs. III A, III B, and III D For the second sample, in Sec. III C, the data are obtained during deposition.

A. Cauchy model

Ψ and Δ, as shown in Fig. 3, are the results of a standard (*ex situ*) SE measurement of our *a*-C:H thin films. The transparent part of the film, characterized by interference fringes in Ψ and Δ, is dependent on the film thickness. This typically goes up to 2.4 eV for a thickness of around 1100 nm. An EMA layer of 50% bulk material and 50% voids is used for the roughness layer. The Cauchy model indicates that this particular sample has a film thickness and surface roughness

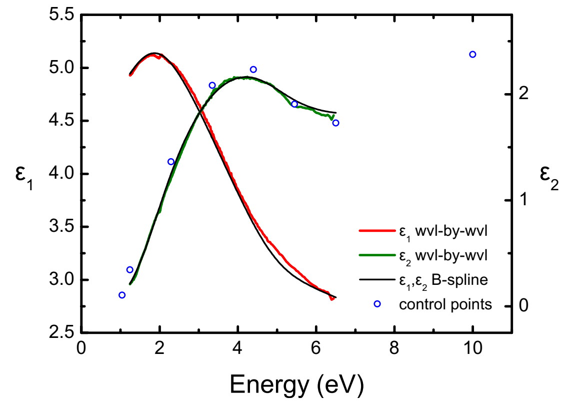

FIG. 4. (Color online) B-spline representation of the dielectric constants ε_1 and ε_2 and the control points for the ε_2 B-spline curve. Twelve knot points are used for ε_2: six equally spaced in the measured range 1.24–6.50 eV and six outside this range at 0.64, 0.84, 1.04, 10, 20, and 21 eV. This means that eight B-spline coefficients are fitted: six for the knots in the measured range and two outside this range at 1.04 and 10 eV. The dielectric spectrum obtained via a wavelength-by-wavelength fit is also plotted for comparison.

of, respectively, 940 and 6 nm. The Cauchy dielectric function is used as a starting point for the B-spline parametrization in the section hereafter.

B. The dielectric function in ambient air

Before ascertaining the (in)homogeneity in depth of the hydrogenated amorphous carbon thin film as deposited by remote plasma deposition, the dielectric function in ambient air of the carbon film will first be determined. This is entirely possible by means of the B-spline model, which makes no assumptions about the physical properties of the deposited film itself.

Throughout the following steps, the roughness layer is included in every fit of the data. Although direct application of the B-spline model is possible, we first apply the Cauchy model to the transparent part of the measured data (see Sec. III A). Optical constants obtained by the Cauchy model are parametrized by B-splines. These B-splines are fitted directly to the experimental data by expanding the data range in steps of 0.5 eV from the band edge onwards to higher energies. If necessary, the number of knots can be decreased to smooth out the dielectric function from the previous step. As a last step, Kramers–Kronig consistency of the B-spline parametrization is enforced (see Sec. II B 2).

The dielectric function, expressed in ε_1 and ε_2, is shown in Fig. 4. Since the dielectric function is Kramers–Kronig consistent, only the spline curve for ε_2 is tabulated (see Table II). The spline curve of ε_2, for this particular sample, is defined by twelve knots and eight coefficients. Six knots are equally spaced between 1.24 and 6.50 eV and six knots are located outside this range at 0.64, 0.84, 1.04, 10, 20, and 21 eV. This means that eight B-spline coefficients are fitted: six for the knots in the measured range and two outside this range at 1.04 and 10 eV. The knots at 10, 20, and 21 eV are used to take into account the absorption outside the measured range. The fit quality (χ^2=3.2) is very good as well. Since a B-spline parametrization is a purely mathematical description of the dielectric function, increasing the number of knots

Downloaded 25 Mar 2010 to 131.155.110.244. Redistribution subject to AIP license or copyright; see http://jap.aip.org/jap/copyright.jsp

TABLE II. B-spline control points for constructing the ε_2 spectrum in ambient air (see also Fig. 4).

Knot position (t_i)	B-spline coefficient (c_i)
0.640	n/a
0.840	n/a
1.040	0.104 34
1.240	0.343 26
2.293	1.363 58
3.345	2.083 41
4.397	2.233 96
5.449	1.906 67
6.501	1.728 61
10.001	2.374 93
20.001	n/a
21.001	n/a

further will reduce χ^2 even more. However, too many knots will only provide a better description of the noise and increase the — probability of — correlation between the coefficients. When using B-splines, a balance should be find between obtaining a low χ^2 value and the number of knots used to reach that value. The drop in χ^2 should be significant, compared to the additional number of knots. Therefore, it is better to provide the absolute minimum number of knots required to obtain a good fit. In addition to the χ^2 value, the correlation r between the fitting parameters should be taken into account. The correlation between the different parameters for this particular sample is shown in Table III. When the threshold for correlation versus no correlation between various parameters is set to $r=0.92$, then there is no correlation between thickness, roughness, and the B-spline coefficients. The B-spline coefficients that fall well within the measured data range show the lowest correlation values. The outer B-spline coefficients (i.e., outside of the measured range), however, do show higher values for the correlation with the B-spline coefficients at the edge of the data range. This is to be expected, since only a few B-spline coefficients contribute to the spline curve for any given wavelength value and the outer B-spline coefficients have no measured data to be compared against. The B-spline dielectric function in Fig. 4 is compared with the dielectric function obtained from the wavelength-by-wavelength fit of Sec. III A. There is a significant overlap between the dielectric function obtained from the wavelength-by-wavelength fit and the B-spline parametrized dielectric function. This overlap between both parametrizations validates the use of the B-spline model for a-C:H films.

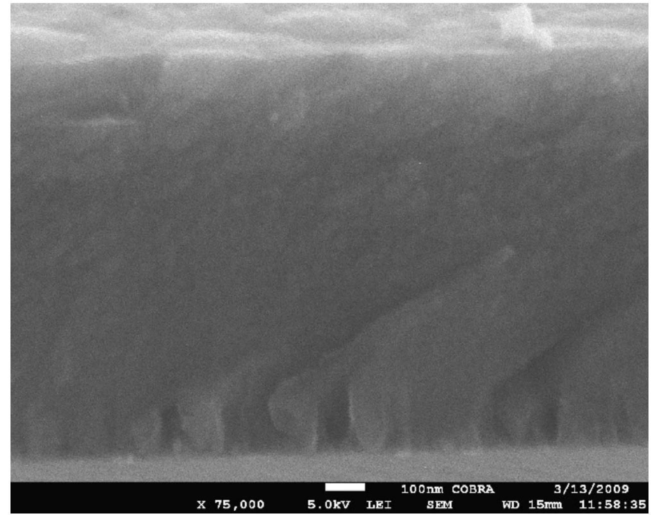

FIG. 5. Cross-sectional SEM image of an a-C:H sample, with magnification 75 000×. Crack lines, due to breaking the sample, are visible.

Together with the dielectric function, SE yields the film thickness and the roughness. With a roughness layer that is at most 1% of the total thickness, the deposited film can be considered smooth. The roughness obtained via SE is compared with an AFM roughness. An AFM (NT-MDT solver P47 with NSG 10 tips), operating in tapping mode to avoid damage to the sample scans a 2×2 μm^2 area with a resolution of 512×512 points. If all the measured heights follow a normal distribution, then the AFM roughness is defined as the standard deviation σ of the height distribution. The AFM and SE roughness are, respectively, 4.9 and 7.6 nm. The proportionality factor between the AFM and SE roughness is 1.55 for this a-C:H sample, whereas Kim *et al.*[23] found a proportionality factor of 2.1. The AFM roughness is in good agreement with the roughness as determined by SE. Cross-sectional SEM (model JEOL 7500FA) measurements (see Fig. 5) of another sample indicates a thickness comparable with a SE thickness of around 1100 nm on average. With the exception of scattered debris near the edge, which was caused by the cutting process, the SEM image (Fig. 6) also

TABLE III. Correlation values between the thickness, roughness and the eight B-spline coefficients, for a-C:H in ambient air (see also Fig. 4).

	Roughness	Thickness	1.04	1.24	2.292	3.345	4.397	5.449	6.501	10.001
Roughness	1	−0.374	0.137	−0.07	−0.402	−0.375	−0.076	−0.056	−0.101	0.437
Thickness	−0.374	1	0.105	−0.124	−0.036	0.131	0.056	−0.048	0.263	−0.473
1.040	0.137	0.105	1	−0.852	0.34	−0.27	0.084	−0.041	−0.075	0.16
1.240	−0.07	−0.124	−0.852	1	−0.551	0.38	−0.167	0.085	0.014	−0.072
2.292	−0.402	−0.036	0.34	−0.551	1	−0.38	0.334	−0.132	0.142	−0.25
3.345	−0.375	0.131	−0.27	0.38	−0.38	1	−0.478	0.273	−0.009	−0.194
4.397	−0.076	0.056	0.084	−0.167	0.334	−0.478	1	−0.571	0.472	−0.415
5.449	−0.056	−0.048	−0.041	0.085	−0.132	0.273	−0.571	1	−0.525	0.291
6.501	−0.101	0.263	−0.075	0.014	0.142	−0.009	0.472	−0.525	1	−0.894
10.001	0.437	−0.473	0.16	−0.072	−0.25	−0.194	−0.415	0.291	−0.894	1

Downloaded 25 Mar 2010 to 131.155.110.244. Redistribution subject to AIP license or copyright; see http://jap.aip.org/jap/copyright.jsp

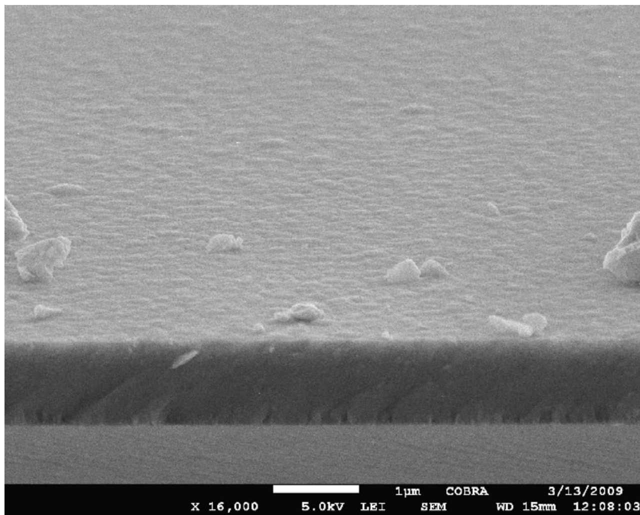

FIG. 6. Cross-sectional SEM image of an a-C:H sample, with magnification 16 000×. The film is uniform and smooth. The large features on the surface are debris from breaking the sample.

shows a uniform, smooth film. The stack of layers visible in the cross section is a validation of the use of our multilayered model.

C. Growth rate and homogeneity in depth of the *a*-C:H film

Assuming linear growth, only the deposition time and thickness after deposition are necessary to calculate a growth rate. From *in situ* SE measurements during deposition, however, also the linearity of the growth rate can be investigated. Also the homogeneity in depth of the deposited film is investigated by comparing the dielectric functions for every measured thickness. If the deposited carbon layer is homogeneous, then the dielectric constants should stay the same throughout the deposition process. *In situ* SE data are therefore gathered with the highest time resolution possible (4.8 Hz). By manually shutting down the plasma source after 32 s in this experiment, the shutter did not block the light path of the ellipsometer and the measurement could continue after the end of the deposition. The *in situ* data have a different wavelength range compared to the *ex situ* data. Therefore, a different set of knots is used (see Table IV for the knot positions). At the moment, limitations in computing power, necessary to calculate the dielectric function for every datapoint, hinder us from performing real time *in situ* analysis. The *in situ* data are therefore analyzed postdeposition. The analysis of these time dependent data occurs stepwise, whereby the dielectric function of the previous datapoint acts as the starting point for the next datapoint. Since the film undergoes nucleation during the initial stages of growth, thickness, roughness, and optical constants are correlated during this stage. Therefore, the data are analyzed backward in time. This allows for a good initial determination of the dielectric function.

TABLE IV. Average of the B-spline control points of the ε_2 spectrum during deposition (see also Fig. 8).

Knot position (t_i)	B-spline coefficient (c_i)
0.152	n/a
0.352	n/a
0.552	0.066 00
0.752	0.001 01
1.828	0.626 02
2.903	1.877 71
3.979	2.229 73
5.054	1.858 46
10.054	1.017 14
20.054	n/a
21.054	n/a

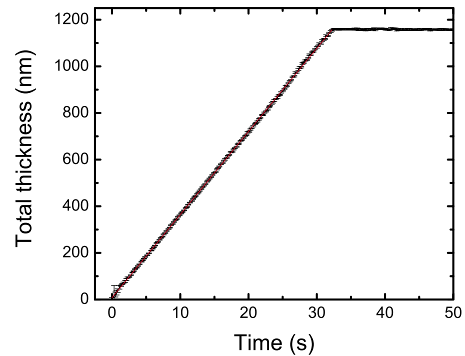

FIG. 7. (Color online) Evolution in total thickness (i.e., thickness plus half of the roughness) during deposition. After 32 s, the plasma is stopped.

Figure 7 shows the total thickness evolution, i.e., $d_{\text{total}} = d + \frac{1}{2} d_{\text{roughness}}$, as a function of deposition time. The void fraction is kept constant at 50%. The growth rate, here defined as the slope of a linear fit of the total thickness, is 35.7 ± 0.1 nm/s. Although the acquisition rate is set to 1 rev/measurement, the actual data are averaged over 4 revs/measurement.[20] With a growth rate of 35.7 nm/s, the film grows with about 7.5 nm during one acquisition interval.

Also the evolution of the ε_2-spectra is plotted (see Fig. 8). These spectra are averaged over the entire deposition interval. Since the B-spline coefficients in the first 4 s (i.e., nucleation) are correlated with the thickness and roughness, these coefficients are excluded from the average. The average of the B-spline coefficients for the ε_2-spectra is tabulated in Table IV. The deviations in ε_2 at energies above 4 eV are

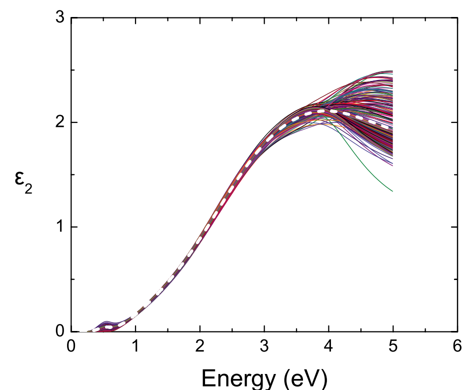

FIG. 8. (Color online) ε_2 spectra during deposition, as determined by the B-spline model. The deviation from the average (dashed line) at higher energies is attributed to relatively larger measurement errors in this energy range.

Downloaded 25 Mar 2010 to 131.155.110.244. Redistribution subject to AIP license or copyright; see http://jap.aip.org/jap/copyright.jsp

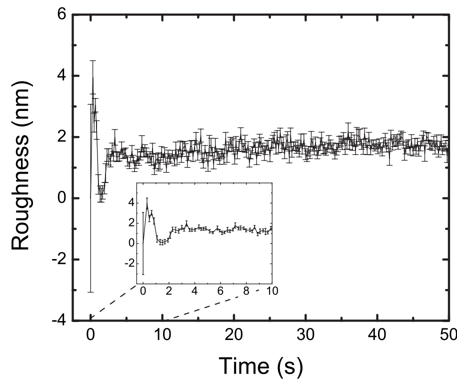

FIG. 9. Evolution in roughness during deposition. The inset shows the nucleation of the film. After 32 s, the plasma is stopped.

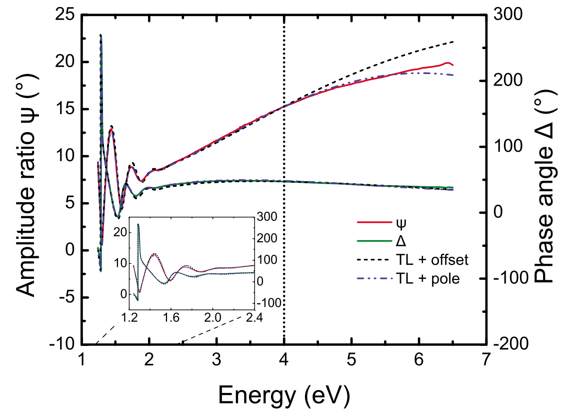

FIG. 10. (Color online) The bulk carbon layer is modeled by a TL oscillator in combination with an offset ε_1 or a pole to account for absorptions outside the measured range. The fit based on a TL oscillator with a pole starts to deviate around 4 eV.

attributed to relatively larger measurement errors in Ψ and Δ for this energy range. With the exception of these deviations above 4 eV, ε_2 remains constant during deposition. The deposited film is therefore considered homogeneous in depth.

Since the deposited *a*-C:H thin film is homogeneous in depth, the dielectric constants — as parametrized by the average B-spline coefficients — can be fixed for every measurement point. Refitting the data with fixed dielectric constants yields, for a second time, the evolution in thickness and roughness. The film thickness, averaged over the time interval from 33 to 48 s, is this time about 1.2% higher. The roughness evolution during deposition is shown in Fig. 9. In the first 3 s of deposition the roughness reaches a maximum of 4 nm, indicating the nucleation process at the start of the deposition. After nucleation, the roughness stays roughly constant at nearly 2 nm.

D. TL oscillator

The mathematically accurate description of the dielectric function, obtained via the B-spline model, is used as a starting point for the parametrization of the bulk layer by one or more TL oscillators. Such a parametrization provides a physical model for the homogeneous carbon bulk layer. Both the SEM and AFM measurements agree well with the layer structure as described for the B-spline model (see Sec. III B). This layer structure is, therefore, reusable in a physics-based model.

Carbon is a band gap material, with a wide gap between the σ valence band and σ^* conduction band and a smaller band gap between the valence and conduction bands of π and π^*, respectively.[2] The π-π^* and σ-σ^* electronic transitions dominate the dielectric function of *a*-C:H (see Fig. 1). Each transition is commonly modeled by a TL oscillator. Although mixing of the π and σ bands occurs in the intermediate energy region between 5 and 8 eV, the resulting π-π^* and σ-σ^* electronic transitions can be neglected.[24]

The same sample as in Sec. III B is reanalyzed. The measurement range of the *ex situ* data is limited by the equipment to a maximum energy of 6.5 eV, which limits us to a single TL oscillator for the π-π^* transition. However, absorptions outside the measured range, in particular, due to the σ-σ^* electronic transition, can be partially taken into account by adding a constant offset to $\varepsilon_2(\omega)$. It is obvious from the fit in Fig. 10, which has a χ^2 of 12.7, that adding a constant offset to ε_1 is only sufficient up to 4 eV. This can be improved by replacing the offset with a pole, which reduces the χ^2 to 5.8. In both variants of this model, the thickness (933 nm) and roughness (6.7 nm) of the layer were first determined by the B-spline model and subsequently fixed. The dielectric function of the carbon layer, as determined by the B-spline model, is then parametrized by a combination of a TL oscillator and an offset ε_∞. The TL parameters obtained in this fit are subsequently used as the starting values for a TL oscillator whereby the offset is replaced with a pole. The parameter space of the global fit (see also Sec. II B 5) for E_{pole} goes from 9 to 20 eV in 24 intervals. The range for A is $0-1000\sqrt{\text{eV}}$ divided in 20 intervals. The results of the fit are shown in Table V. In contrast with the B-spline model, the TL oscillator with a pole also provides physical information about the carbon film. The TL oscillator describes the π-π^* transition, whereas the pole indicates the location of the σ-σ^* electronic transition. The B-spline model is thus used as a stepping stone to a physics-based model, from which additional information about the bulk layer can be extracted.

IV. DISCUSSION

We have shown that hydrogenated amorphous carbon thin films, as deposited by remote plasma deposition, can be

TABLE V. The dielectric function of an *a*-C:H thin film is parametrized by a TL oscillator, with two variations. In the first variant, the σ-σ^* transition is represented by an offset. In the second variant, the offset is replaced with a pole. The same sample was also analyzed by the B-spline model, which gave a χ^2 of 3.2.

Parameter	TL+ε_∞	TL+pole
χ^2	12.7	5.8
A_π	20.4 eV	21.0 eV
Γ_π	7.19 eV	6.64 eV
$E_{0\pi}$	5.08 eV	4.69 eV
E_g	0.780 eV	0.818 eV
ϵ_∞	2.73 eV	n/a
A_{pole}	n/a	195 eV
E_{pole}	n/a	11.0 eV

Downloaded 25 Mar 2010 to 131.155.110.244. Redistribution subject to AIP license or copyright; see http://jap.aip.org/jap/copyright.jsp

represented by a fairly simple and straightforward set of layers. The first two layers are the substrate itself, consisting of a (semi-infinite) Si wafer of 1 mm thick and a native oxide layer of 1.6 nm. Layer 3 is the homogenous bulk carbon layer. The fourth and last layer is the roughness of the film, which is described by Bruggeman's EMA with a mix of 50% voids and 50% bulk material. We have verified this layer structure by cross-sectional SEM and AFM measurements.

The B-spline model, which was instrumental in determining the film thickness and roughness, also provides an excellent method to determine the dielectric function of the carbon film throughout the deposition, although only for postdeposition analysis. The average of the dielectric function shows a tail below 0.7 eV, outside of the measured wavelength range. Although the B-spline parametrization of ε_2 goes smoothly to zero within the measured wavelength range, it accomplishes this at the expense of the wavelengths outside of the measured range. This tail is, therefore, an artifact of the mathematical representation of ε_2. The B-spline parametrization can only accurately represent the available data. Extrapolation to wavelengths outside of the measured range is thus not possible, as illustrated by the tail below 0.7 eV. The evolution of the dielectric function was used to establish the homogeneity in depth of the *a*-C:H layer. Since the film is homogeneous, the average dielectric constants should be used when determining the thickness evolution during growth. However, the difference in thickness is about 1.2% when the dielectric constants are included in the fit. Fixing the dielectric constants to the average value is, therefore, not necessary to get a good determination of the thickness evolution. Previous studies on the growth of *a*-C:H under similar deposition conditions on the same setup used infrared interferometry to determine the growth rate.[25,26] The rate found by Gielen *et al.* is comparable to what we found by means of *in situ* SE. Our analysis shows a deposition rate of about 36 nm/s. Even though the integrated thickness during one acquisition interval is 7.5 nm, the *in situ* data acquisition was fast enough to observe the nucleation stage of the film, which lasted no more than 3 s. With a roughness layer thinner than 1% of the total thickness, the film can be considered smooth.

The B-spline model served as a stepping stone for a physics-based model. In this model, the dielectric function is parametrized by means of a TL oscillator in combination with either an offset or a pole. Although the TL oscillator with a pole is based on a physical model, it is computationally slower than the mathematical approach via the B-spline model. Moreover, the B-spline model is less susceptible to correlation between the different fitting parameters. Therefore, if only the dielectric spectrum in the measured wavelength range and a fast and accurate thickness determination are of primary concern to the experimentalist, the B-spline model is recommended for hydrogenated amorphous carbon thin films. Application of the B-spline model is, however, not limited to hydrogenated amorphous carbon thin films.[14] The B-spline model is also suitable for *in situ* monitoring the growth of, e.g., μc-silicon. The change from *a*-silicon to μc-silicon has a clear distinction in the dielectric function. It is envisaged that in due time, due to the ever increasing CPU computing speed, the B-spline method can be used to monitor real time the changes in the dielectric function of *a*-C:H *in situ*, during deposition or etching.

V. CONCLUSION

We have shown the versatility of the B-spline model as a tool in the analysis of *a*-C:H thin films. We concluded that the deposited film is smooth and homogeneous in depth. The B-spline model can serve as a stepping stone to more physical models such as the TL oscillator. The expanding thermal plasma deposition technique has a high and constant deposition rate. In all, the B-spline model is an accurate and fast method to determine thickness, roughness, and dielectric constants of — as has been shown — hydrogenated amorphous carbon thin films, both for *ex situ* and *in situ* measurements.

ACKNOWLEDGMENTS

We would like to thank W. Keuning for the SEM measurements and V. Vandalon for the AFM measurements. We also greatly appreciate the skillful technical assistance of M. J. F. van de Sande, J. J. A. Zeebregts, and H. M. M. de Jong. This work is part of the research program of the Dutch Foundation for Fundamental Research on Matter (FOM-TFF). It is also supported by the European Communities under the contract of Association between EURATOM and FOM and carried out within the framework of the European Fusion Programme.

[1] J. W. A. M. Gielen, W. M. M. Kessels, M. C. M. van de Sanden, and D. C. Schram, J. Appl. Phys. **82**, 2643 (1997).
[2] J. Robertson, Mater. Sci. Eng., R. **37**, 129 (2002).
[3] J. Benedikt, K. G. Y. Letourneur, M. Wisse, D. C. Schram, and M. C. M. van de Sanden, Diamond Relat. Mater. **11**, 989 (2002).
[4] S. V. Singh, M. Creatore, R. Groenen, K. Van Hege, and M. C. M. van de Sanden, Appl. Phys. Lett. **92**, 221502 (2008).
[5] H. Fujiwara, *Spectroscopic Ellipsometry: Principles and Applications* (John Wiley & Sons Ltd., Chichester, UK, 2007).
[6] *Handbook of Ellipsometry*, edited by H. G. Thompkins and E. Irene (William Andrew Inc., Norwich, New York, 2005).
[7] E. Langereis, S. B. S. Heil, H. C. M. Knoops, W. Keuning, M. C. M. van de Sanden, and W. M. M. Kessels, J. Phys. D **42**, 073001 (2009).
[8] S. Kassavetis, P. Patsalas, S. Logothetidis, J. Robertson, and S. Kennou, Diamond Relat. Mater. **16**, 1813 (2007).
[9] S. Logothetidis, Diamond Relat. Mater. **12**, 141 (2003).
[10] S. S. Zumdahl, *Chemical Principles*, 3rd ed. (Houghton Mifflin, Boston, MA, 1998).
[11] G. E. Jellison and F. A. Modine, Appl. Phys. Lett. **69**, 371 (1996).
[12] J. Fink, T. Müller-Heinzerling, J. Pflüger, B. Scheerer, B. Dischler, P. Koidl, A. Bubenzer, and R. Sah, Phys. Rev. B **30**, 4713 (1984).
[13] S. Waidmann, M. Knupfer, J. Fink, B. Kleinsorge, and J. Robertson, J. Appl. Phys. **89**, 3783 (2001).
[14] B. Johs and J. S. Hale, Phys. Status Solidi A **205**, 715 (2008).
[15] D. Aspnes, Thin Solid Films **89**, 249 (1982).
[16] A. von Keudell and W. Jacob, J. Appl. Phys. **79**, 1092 (1996).
[17] M. C. M. van de Sanden, G. M. Janssen, J. M. de Regt, D. C. Schram, J. A. M. van der Mullen, and B. van der Sijde, Rev. Sci. Instrum. **63**, 3369 (1992).
[18] G. M. W. Kroesen, D. C. Schram, and J. C. M. de Haas, Plasma Chem. Plasma Process. **10**, 531 (1990).
[19] J. W. A. M. Gielen, M. C. M. van de Sanden, P. R. M. Kleuskens, and D. C. Schram, Plasma Sources Sci. Technol. **5**, 492 (1996).
[20] J. A. Woollam Co, Inc., personal communication 6 July (2009).
[21] A change in one of the c_i coefficients affects the next four segments, as can be seen from the recursive formula.

Downloaded 25 Mar 2010 to 131.155.110.244. Redistribution subject to AIP license or copyright; see http://jap.aip.org/jap/copyright.jsp

[22]J. A. Woollam Co., Inc., CompleteEASE TM software manual, version 3.18 ed. (2007).
[23]I.-Y. Kim, S.-H. Hong, A. Consoli, J. Benedikt, and A. von Keudell, J. Appl. Phys. **100**, 053302 (2006).
[24]N. Savvides, J. Appl. Phys. **59**, 4133 (1986).
[25]J. W. A. M. Gielen, M. C. M. van de Sanden, and D. Schram, Appl. Phys. Lett. **69**, 152 (1996).
[26]J. W. A. M. Gielen, P. R. M. Kleuskens, M. C. M. van de Sanden, L. J. van Ijzendoorn, D. C. Schram, E. H. A. Dekempeneer, and J. Meneve, J. Appl. Phys. **80**, 5986 (1996).

Downloaded 25 Mar 2010 to 131.155.110.244. Redistribution subject to AIP license or copyright; see http://jap.aip.org/jap/copyright.jsp